

Vickers hardness indentation size effect in selective laser melted MSI maraging steel

Sebastian Balos¹, Dragan Rajnovic¹, Leposava Sidjanin¹,
Olivera Eric Cekic², Slobodan Moraca¹, Mirjana Trivkovic¹ 
and Milan Dedic³

Proc IMechE Part C:
J Mechanical Engineering Science
0(0) 1–7
© IMechE 2019
Article reuse guidelines:
sagepub.com/journals-permissions
DOI: 10.1177/0954406219892301
journals.sagepub.com/home/pic



Abstract

In this paper, selective laser melting fabricated specimens in non-heat-treated and heat-treated conditions were subjected to Vickers microhardness testing, by using a full range of loadings: 10, 25, 50, 100, 200, 300, 500, and 1000 g. Microhardness of longitudinal sections and cross-sections were correlated and the obtained values were plotted against loadings and indentation size effect was studied, in order to find the optimal loading range, that gives the material true microhardness, or load-independent hardness. The load dependence of the measured Vickers hardness values was described quantitatively through the application of the Meyer's law, proportional specimen resistance, and the modified proportional specimen resistance model. It was found that the microhardness rises as the loading is higher, causing a reversed indentation size effect, clearly indicating the range of true hardnesses of the tested material. Also, proportional specimen resistance and modified proportional specimen resistance models were found to have the highest correlation factors indicating their higher adequacy compared to Meyer's prediction model.

Keywords

Direct selective laser melting, Vickers microhardness, indentation size effect, maraging steel

Date received: 8 October 2018; accepted: 11 November 2019

Introduction

Selective laser melting (SLM) is a type of additive manufacturing (AM) technologies. Today, over 30 different types of AM have been developed, with a great variety between principles, materials, and effects.^{1,2} SLM technology uses the basic principle of layered building of the manufactured part without tools, fed by a computer-aided design (CAD) model. This model is split into two-dimensional layers of micron-sized powder, joined by laser. That means, a huge potential exists, in terms of flexibility, production of complex and thin-walled parts, no need for a mold, relatively short production time, high resolution, minimal post processing in terms of machining and different materials used, ranging from metals, polymers, and ceramics.^{3–5} However, there are several important drawbacks that limit the practical application of SLM technology. Some of them are as follows: warping and cracking of parts, thermal stresses, detrimental tensile residual stresses, undesirable microstructure occurrence, shrinking-induced residual stresses, particularly of tensile nature on the surface, as well as lower mechanical properties compared to conventionally fabricated parts, lower fatigue resistance.^{1,6,7} A great deal of attention has been paid to

the characterization of SLM fabricated parts obtained with optimized parameters with or without heat treatment. Fatigue, hardness, and tensile properties were usually correlated to metallographic features of the material as is the case with conventionally fabricated specimens.^{8–13}

The determination of tensile properties, fatigue, and microstructure is well established and covered with standards and procedures. However, it is not the case with hardness and microhardness. The literature survey reveals that although the most widely used, Vickers microhardness should be used carefully, due to the nonhomogenous nature of the material. Namely, the SLM technology fuses the powder by laser irradiation, creating the locally melted material,

¹Faculty of Technical Sciences, University of Novi Sad, Novi Sad, Serbia

²Innovation Centre, Faculty of Mechanical Engineering, University of Belgrade, Belgrade, Serbia

³Faculty of Mechanical and Civil Engineering in Kraljevo, University of Kragujevac, Kraljevo, Serbia

Corresponding author:

Mirjana Trivkovic, Faculty of Technical Sciences, University of Novi Sad, Novi Sad 21000, Serbia.

Email: mirjana.trivkovic@uns.ac.rs

along with a thin heat-affected zone around the melt pool in the previous layer.^{14,15} Several studies used a different Vickers microhardness loading. In the study done by Ryniewicz et al., 200 g Vickers microhardness loading was used on Ti-6Al-4V alloy.¹³ The same material was tested by Vickers microhardness loading of 300 g in the research done by Campanelli et al.¹⁶ The same loading was used in the study by Zaharia et al. when testing 316-type stainless steel honeycombs manufactured by SLM technology.¹⁷ Nakamoto et al. studied the microhardness of carbon steels S33C, S50C, S75C, and S105C by using 500 g Vickers microhardness loading.¹⁸ A total of 200 g loading Knoop microhardness was used to test SLM melted iron and tungsten powders in the study done by Nie et al.¹⁹ However, perhaps the most comprehensive is the study done by Dobransky et al. on MS1 maraging steel, by using Vickers hardness with different loadings: 10, 25, 50, 100, 200, 300, 500, and 1000 g, but without determining the load-independent hardness (H_{LIH}).²⁰ Clearly, there is hardly a consensus not only on Vickers hardness optimal loading, but also on the hardness measurement methodology. This clearly makes the comparison of different results obtained in various studies difficult, unreliable, if not impossible.²¹ It can be overcome by considering the indentation size effect (ISE), which represents a phenomenon that may be briefly described as an indentation-depth-dependent hardness.²² Namely, by the application of different loads, various microhardnesses are obtained. Usually, a lower indentation depth results in an increased hardness.²³ The ISE was observed in ceramic, metallic, and polymer materials.²¹ The ISE in metals may be related to plastic deformation and dislocation movement effects increasing flow stress and hardness values.^{24,25} This occurs at indentation depths smaller than approximately 0.2 μm . However, the roughness of the material surface can influence the deformation mechanisms and hardness values.^{26,27} In this study, an attempt was made to study the ISE effect in SLM fabricated parts and find the optimized Vickers microhardness loading corresponding to the load independent hardness (H_{LIH}).

Experimental

The experimental work was conducted on the EOSINT M280 SLM device, equipped with 200 W continuous wave Ytterbium laser, emitting 0.2032 mm thick and 1064 nm infra-red beam, with a scan speed of 7000 mm/s in nitrogen environment. Device working space was 250 \times 250 mm² with a height of 325 mm.

The material was supplied by EOS: maraging steel MS1 (1.2709, X3NiCoMoTi18-9-5), with nominal chemical composition given in Table 1.

Specimens obtained by SLM process, used in this study were in accordance to ISO 1143 standard (Figure 1). Specimens have been built in vertical stacking direction with respect to the horizontal base plate. Specimens were detached from the base plate by wire-cut electrical discharge machining (EDM). Afterwards, specimens underwent surface cleaning by microshot-peening by 400 μm stainless steel spheres. Then, three specimens were left nitrated (N), while three were heat treated by aging up to 490 $^{\circ}\text{C}$ for 6 h, as recommended by the material manufacturer.

Specimens were sectioned in the longitudinal plane and the cross plane to reveal the laser fused material in two sections. Sectioning was done on a specialized grind cutter with emulsion cooling. Then, specimens were mounted in polyethylene and ground with a set of SiC abrasive papers: 150, 220, 320, 400, 500, 600, 800, 1000, 1500, and 2000. After that, polishing with 6, 3, 1, and $\frac{1}{4}$ μm diamond suspensions was conducted. Microstructures were revealed by etching, by using aqua regia. After evaluating microstructures on Leitz Orthoplan light microscope, the same specimens were used for microhardness testing. Vickers microhardness was measured by Wilson Tukon 1102 device, with loadings of 10, 25, 50, 100, 200, 300, 500, and 1000 g. An attempt was made to test individual melted areas, rounded or elongated, depending on the plate observed, the results were compared and hardness-loading charts were created for heat-treated cross plane (HC) and longitudinal plane (HL), as well as non-heat-treated cross plane (NC) and longitudinal plane (NL).

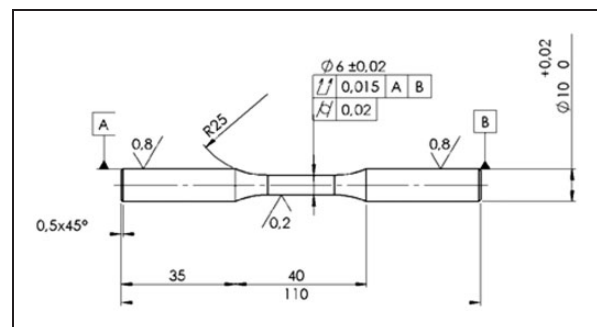


Figure 1. Specimen dimensions in accordance to ISO 1143 standard.

Table 1. MS1 maraging steel composition (mass%).

Ni	Co	Mo	Ti	Al	Cr	Cu	C	Mn	Si	P	S	Fe
17–19	8.5–9.5	4.5–9.2	0.6–0.8	0.05–0.15	≤0.5	≤0.5	≤0.03	≤0.1	≤0.1	≤0.01	≤0.01	Balance

The load dependence of the measured Vickers hardness values was also described quantitatively through the application of the classic Meyer's law, proportional specimen resistance (PSR), and the modified PSR model.

The classical Meyer's law has the following form

$$P = Ad^n \quad (1)$$

where P is the indentation load and d the resulting indentation size. The parameter A and n are values that can be derived directly from the curve fitting of the experimental data.²⁸

An alternative to the Meyer's law is proportional specimen resistance (PSR) model based on equation (2)

$$P = a_1d + a_2d^2 \quad (2)$$

where a_1 and a_2 are experimental constants.

The modified PSR model proposed by Gong and Li²⁸ who found that the surface of the specimen is exposed to the stress, found that this stress was induced by specimen preparation, mostly grinding,

necessary for microhardness test. The modified PSR model can be described as follows

$$P = P_0 + a_1d + a_2d^2 \quad (3)$$

where P_0 is the experimental constant, while a_1 and a_2 are experimental constants, as in equation (2).

Results and discussion

Microstructures of SLM fabricated specimens are shown in Figure 2. In longitudinal sectioned specimens, a short rounded-scale-like melted areas are present, as a result of cross-sectioned laser-melted passes (Figure 2(a) and (c)). On the other hand, in Figure 2(b) and (d), cross-section of the SLM fabricated specimens is presented, with elongated areas representing laser melted passes.

The results of Vickers microhardness measurements are shown in Figure 3. The presented charts show a pronounced ISE, particularly in specimens NC, HC, and HL. A more pronounced differences

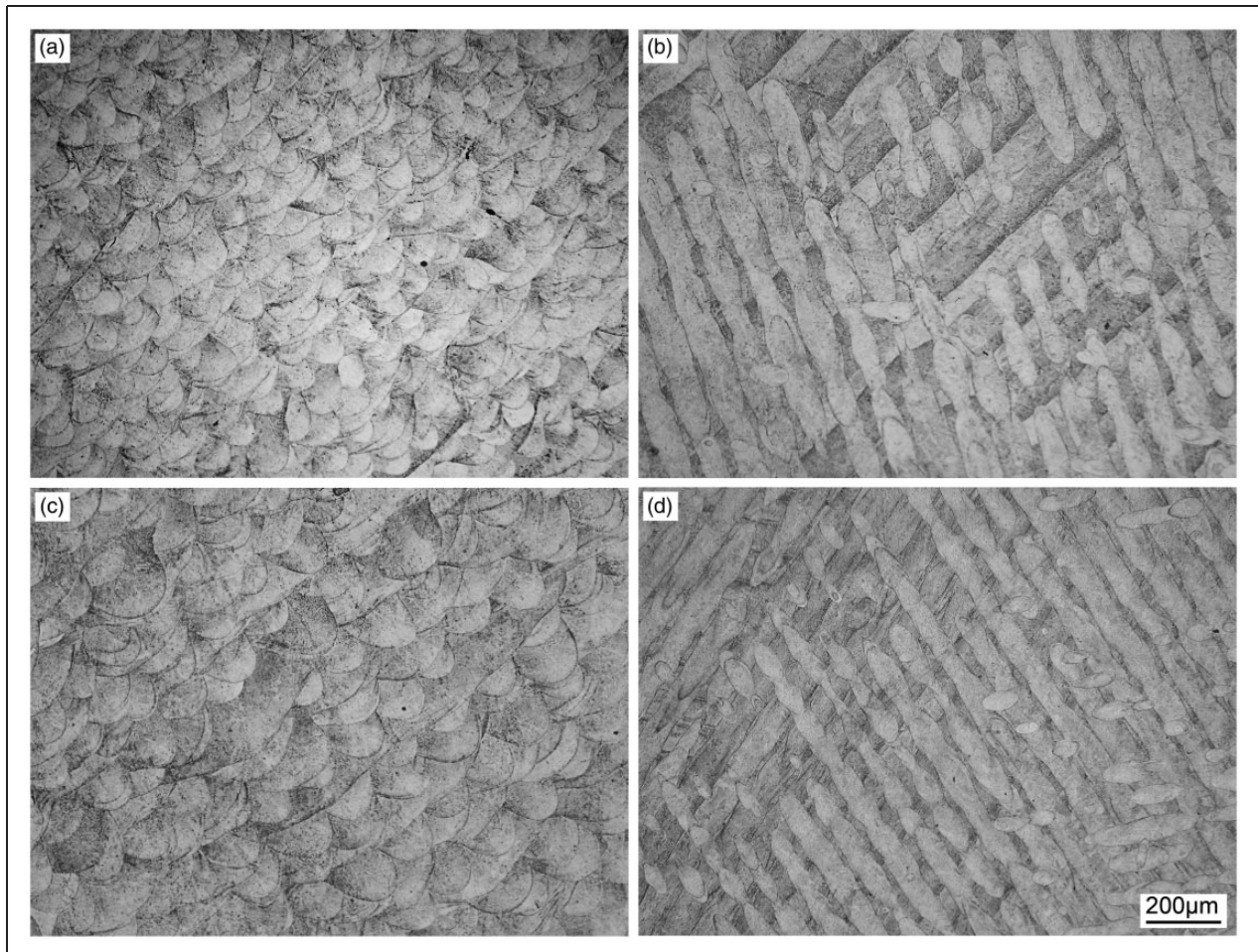


Figure 2. Microstructures of SLM fabricated specimens: (a) NL; (b) NC; (c) HL; (d) HC.

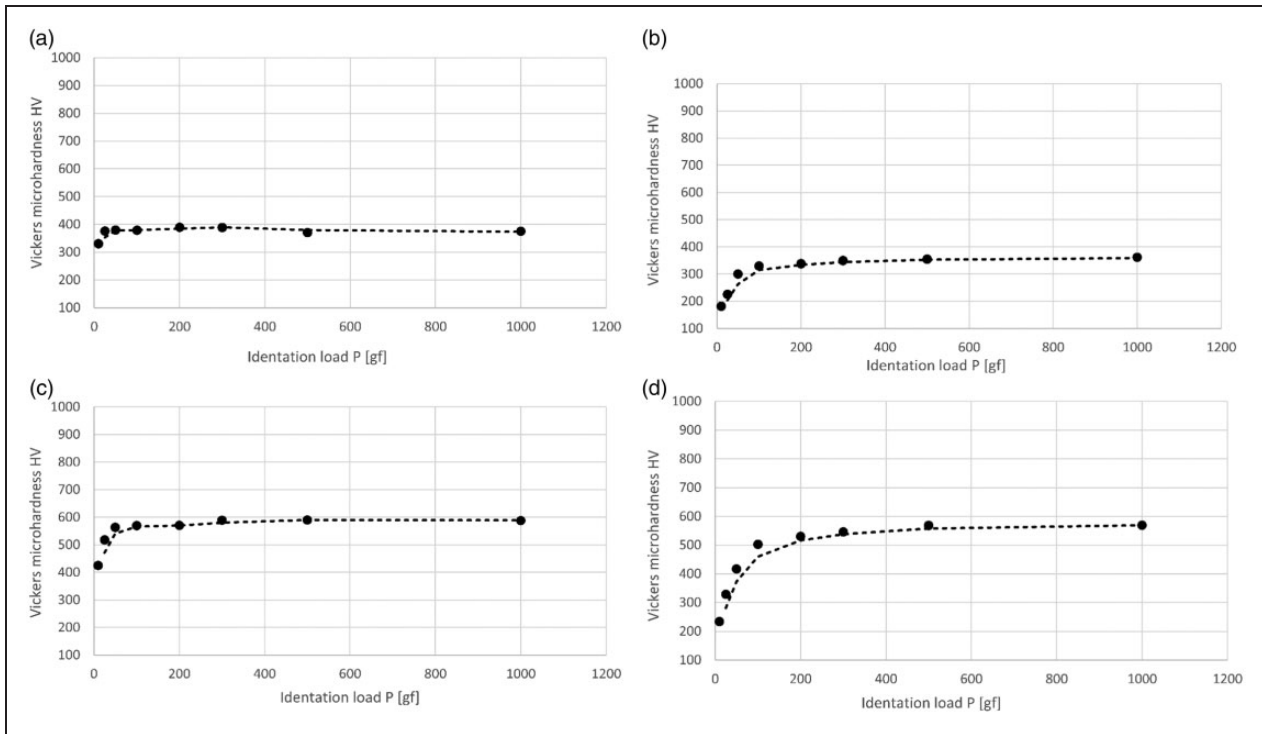


Figure 3. Vickers microhardness of specimen: (a) NL; (b) NC; (c) HL; (d) HC.

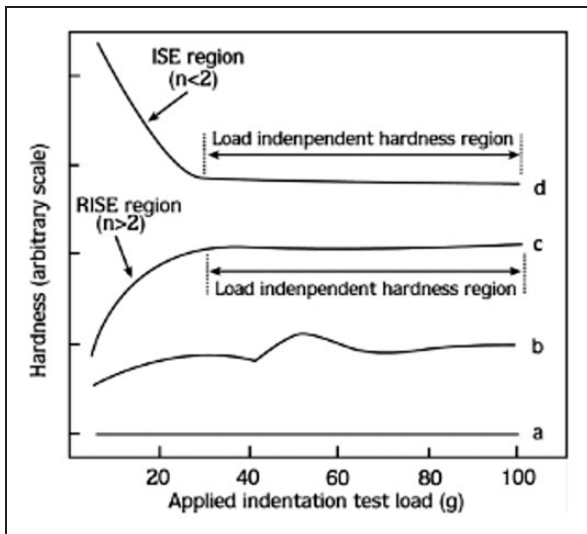


Figure 4. Hardness ISE variations.²⁸

ISE: indentation size effect; RISE: reverse indentation size effect.

in Vickers microhardness were found to exist in NC, compared to HC and HL. In specimen NL, a much less pronounced ISE can be observed. In all specimens, the microhardness value increases with increase in load, which is called the reversed indentation size effect (RISE).

This behavior is one of the four common so far reported²⁹ (Figure 4). In Figure 4(a)-type variation, the hardness is approximately constant with respect to load. In this type of variation, an ideal instrument

and material response is found.⁵ Maximum and minimum values are found in Figure 4(b)-type variation. This type of behavior was found in some organic crystals and polymers.³⁰ The behavior as in Figure 4(c) is called the RISE and is found in this study. It is characterized by a rise in hardness as the load is increased. Finally, in Figure 4(d), ISE effect is present, where the hardness is decreased as the load is higher.³¹ Sometimes, in case of brittle polymers or ceramics, the occurrence of cracks may compromise the accuracy of the diagonal size measurement.²²

In Figure 4, the load-independent hardness region is indicated (H_{LIH}), in ISE and RISE curves (Figure 4(c) and (d)). The results obtained in its study, shown in Figure 3, with an input from Figure 3(c), suggest that the H_{LIH} value for SLM fabricated non-heat-treated specimen (NL, NC) is in the region of 350–370 HV and test load must be over 200 g. A similar optimal load range can be recommended for heat treated specimens, with microhardness in the region of 530–580 HV.

The load dependence of the measured Vickers hardness values described quantitatively through the application of the Meyer's law, proportional specimen resistance (PSR), and the modified PSR model is shown in Figures 5 to 7 and Tables 2 to 4. In Table 2 and Figure 5, Meyer's law parameters are presented, along with correlation factor, which, if closer to 1, means a better fit of the mathematical model to obtained results. The power law exponent is over 2 and is higher in specimens NL and HL, indicating a less pronounced ISE effect compared to NC and HC specimens as well as some kinds of polymers,

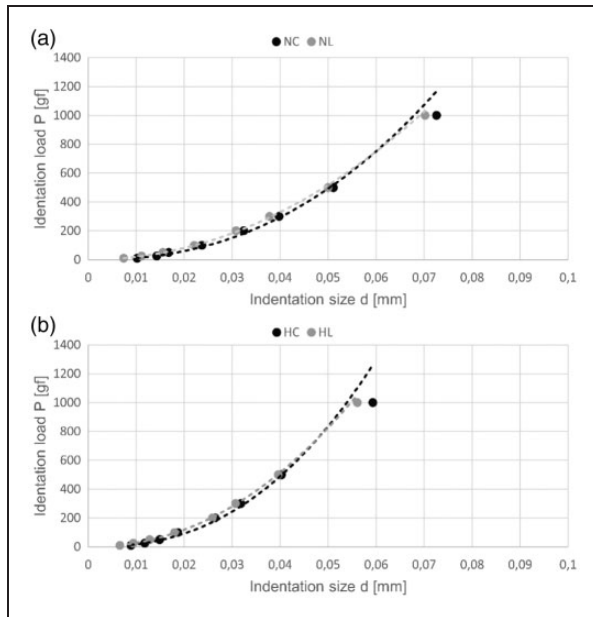


Figure 5. Correlation between P and d in accordance to Meyer's model: (a) non-heat-treated; (b) heat-treated. NL: non-heat-treated longitudinal plane; NC: non-heat-treated cross plane; HL: heat-treated longitudinal plane; HC: heat-treated cross plane.

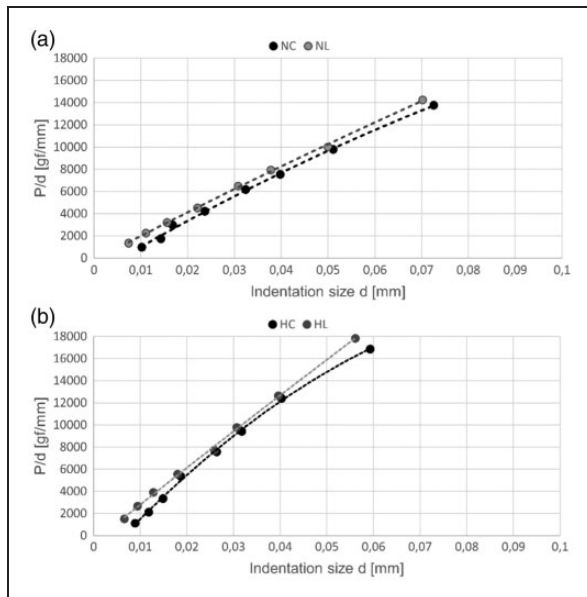


Figure 6. Correlation between P/d and d in accordance to PSR model: (a) non-heat-treated; (b) heat-treated. NL: non-heat-treated longitudinal plane; NC: non-heat-treated cross plane; HL: heat-treated longitudinal plane; HC: heat-treated cross plane.

including microwave-post polymerized PMMA.²² These results are in accordance to the results presented in Figure 3.

In Figure 6 and Table 3, the results of the linear PSR model are presented. Correlation factors R^2 are higher than in Meyer's model, indicating a higher adequacy in predicting microhardness values.

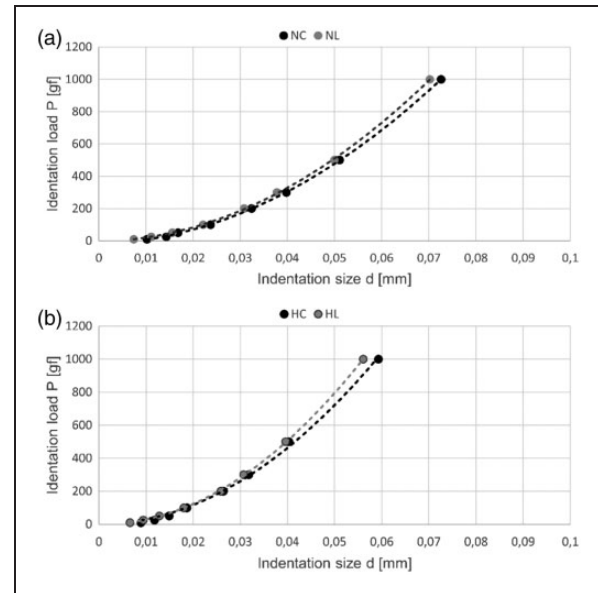


Figure 7. Correlation between P and d in accordance to modified PSR model: (a) non-heat-treated; (b) heat-treated. mmNL: non-heat-treated longitudinal plane; NC: non-heat-treated cross plane; HL: heat-treated longitudinal plane; HC: heat-treated cross plane.

Table 2. Regression analysis of the experimental data according to Meyer's model.

Specimen	A	log A	n	Correlation factor (R^2)
NL	501,028	5.670	2.3116	0.9903
NC	227,931	5.3578	2.0321	0.9994
HL	1.00E+06	6.000	2.4092	0.9875
HC	473,266	5.6751	2.1200	0.9982

NL: non-heat-treated longitudinal plane; NC: non-heat-treated cross plane; HL: heat-treated longitudinal plane; HC: heat-treated cross plane.

Table 3. Regression analysis of the experimental data according to the PSR model.

Specimen	a_1	a_2	Correlation factor (R^2)
NL	251,468	-583,717	0.9981
NC	219,960	-218,887	0.9992
HL	460,833	-2.00E+06	0.9986
HC	338,628	-186836	0.9990

NL: non-heat-treated longitudinal plane; NC: non-heat-treated cross plane; HL: heat-treated longitudinal plane; HC: heat-treated cross plane.

The modified PSR model results, proposed by Gong and Li are shown in Figure 7 and Table 4.²⁹ This model considers the material surface features such as stress induced by specimen preparation,

Table 4. Regression analysis of the experimental data according to the modified PSR model.

Specimen	P_0	a_1	a_2	Correlation factor (R^2)
NL	-19.147	808.43	182,312	0.9999
NC	-3.221	378.94	197,655	0.9998
HL	-48.206	3404	242,005	0.9993
HC	-2.7472	-130.57	321,364	0.9875

NL: non-heat-treated longitudinal plane; NC: non-heat-treated cross plane; HL: heat-treated longitudinal plane; HC: heat-treated cross plane.

necessary for conducting metallographic and hardness tests. Correlation factors (R^2) are similar to those obtained by the PSR model and higher than those obtained by Meyer's model, indicating a closer fit between predicted and measured values. The fact that correlation factors are similar in PSR and modified PSR models, the surface tension as the result of specimen preparation is relatively low, unlike the results obtained by Balos et al. on PMMA polymer.²¹ Obviously, mechanical properties of polymer are significantly lower, and the effect of grinding and polishing is much more pronounced compared to maraging steel.

Conclusions

In accordance to the results obtained in this study, the following conclusions can be drawn:

- Vickers microhardness of the specimen is highly dependent on loading. It was found that the microhardness rises as the loading is higher, causing a RISE.
- Obtained values are dependent also on the direction of specimen sectioning. A narrower range of results was obtained when a longitudinal section was tested, that is, the section that reveals rounded areas, solidified during fabrication.
- Optimal Vickers microhardness loading for tested non-heat-treated and heat-treated specimens is at least 200 g, which provides comparable microhardness values measured in longitudinal and cross planes of the specimen, that is, in the rounded areas and elongated areas of the specimen.
- Microhardness described quantitatively through the application of the Meyer's law, PSR, and the modified PSR model prediction. The highest adequacies, that is, correlation factors were obtained by applying a PSR and modified PSR models.
- True microhardness, that is, load-independent hardness of tested specimens (H_{LIH}) are: non-heat-treated specimens 350–370 HV and 530–580 HV for heat-treated specimens.

Before microhardness testing, a careful optimization of test indentation load is needed to reveal the

optimal values and true, load-independent hardness H_{LIH} . To determine the optimal load, conducting a pre-experiment is needed.


Declaration of Conflicting Interests

The author(s) declared no potential conflicts of interest with respect to the research, authorship, and/or publication of this article.

Funding

The author(s) disclosed receipt of the following financial support for the research, authorship, and/or publication of this article: This paper represents a part of research performed within the project "Advanced design rules for optimal dynamic properties of additive manufacturing products – A_MADAM", which received funding from the European Union's Horizon 2020 research and innovation programme under the Marie Skłodowska-Curie grant agreement no.734455.

ORCID iD

Mirjana Trivkovic  <https://orcid.org/0000-0002-9823-1426>

References

1. Kalentics N, Boillat E, Peyre P, et al. Tailoring residual stress profile of selective laser melted parts by laser shock peening. *Addit Manuf* 2017; 16: 90–97.
2. Levy GN, Schindel R and Kruth JP. Rapid manufacturing and rapid tooling with layer manufacturing (LM) technologies, state of the art and future perspectives. *CIRP Ann - Manuf Technol* 2017; 52: 589–609.
3. Ćirić-Kostić S, Bogojević N and Vranić A. Machining and heat treatment effects on the fatigue properties of Maraging steel produced by DMLS. In: *IX international conference "Heavy Machinery-HM 2017"*, Zlatibor, 2017.
4. Abe F, Osakada K, Shiomi M, et al. The manufacturing of hard tools from metallic powders by selective laser melting. *J Mater Process Technol* 2001; 111: 210–213.
5. Constantnidis G, Tomlinson RD and Neumann H. Microhardness of CuInSe₂. *Philos Mag Lett* 1988; 57: 91–97.
6. Kunze K, Etter T, Grässlin J, et al. Texture, anisotropy in microstructure and mechanical properties of IN738LC alloy processed by selective laser melting (SLM). *Mater Sci Eng A* 2014; 620: 213–222.
7. Kempen K, Vrancken B, Buls S, et al. Selective laser melting of crack-free high density M2 high speed steel parts by baseplate preheating. *J Manuf Sci Eng* 2014; 136: 061026.
8. Croccolo D, De Agostinis M, Fini S, et al. Influence of the build orientation on the fatigue strength of EOS maraging steel produced by additive metal machine. *Fatigue Fract Eng Mater Struct* 2016; 39: 637–647.
9. Croccolo D, De Agostinis M, Fini S, et al. Sensitivity of direct metal laser sintering Maraging steel fatigue strength to build orientation and allowance for machining. *Fatigue Fract Eng Mater Struct* 2019; 42: 374–386.
10. Croccolo D, De Agostinis M, Fini S, et al. Effects of build orientation and thickness of allowance on the fatigue behaviour of 15–5 PH stainless steel manufactured by DMLS. *Fatigue Fract Eng Mater Struct* 2018; 41: 900–916.

11. Yasa E, Kempen K, Kruth J-P, et al. Microstructure and mechanical properties of maraging steel 300 after selective laser melting. In: *Solid freeform fabrication symposium proceedings*, 2010, pp.383–396..
12. Kempen K, Yasa E, Thijs L, et al. Microstructure and mechanical properties of selective laser melted 18Ni-300 steel. *Phys Procedia* 2011; 12: 255–263.
13. Ryniewicz AM, Bojko Ł and Ryniewicz WI. Microstructural and micromechanical tests of titanium biomaterials intended for prosthetic reconstructions. *Acta Bioeng Biomech* 2016; 18: 111–117.
14. Shifeng W, Shuai L, Qingsong W, et al. Effect of molten pool boundaries on the mechanical properties of selective laser melting parts. *J Mater Process Technol* 2014; 214: 2660–2667.
15. Chlebus E, Kuźnicka B, Kurzynowski T, et al. Microstructure and mechanical behaviour of Ti-6Al-7Nb alloy produced by selective laser melting. *Mater Charact* 2011; 62: 488–495.
16. Campanelli SL, Contuzzi N, Ludovico AD, et al. Manufacturing and characterization of Ti6Al4V lattice components manufactured by selective laser melting. *Materials (Basel)* 2014; 7: 4803–4822.
17. Zaharia SM, Lancea C, Chicco LA, et al. Mechanical properties and corrosion behaviour of 316L stainless steel honeycomb cellular cores manufactured by selective laser melting. *Trans FAMENA* 2018; 41: 11–24.
18. Nakamoto T, Shirakawa N, Miyata Y, et al. Selective laser sintering of high carbon steel powders studied as a function of carbon content. *J Mater Process Technol* 2009; 209: 5653–5660.
19. Nie B, Yang L, Huang H, et al. Femtosecond laser additive manufacturing of iron and tungsten parts. *Appl Phys A Mater Sci Process* 2015; 119: 1075–1080.
20. Dobránský J, Baron P, Simkulet V, et al. Examination of material manufactured by direct metal laser sintering (DMLS). *Metalurgija* 2015; 54: 477–480.
21. Balos S, Sidjanin L and Pilic B. Indentation size effect in autopolymerized and microwave post treated poly(methyl methacrylate) denture reline resins. *Acta Polytech Hungarica* 2014; 11: 239–249.
22. Han CS and Nikolov S. Indentation size effects in polymers and related rotation gradients. *J Mater Res* 2007; 22: 1662–1672.
23. Zamfirova G and Dimitrova A. Some methodological contributions to the Vickers microhardness technique. *Polym Test* 2000; 19: 533–542.
24. Ma Q and Clarke DR. Size dependent hardness of silver single crystals Size dependent hardness of silver single crystals. *J Mater Res* 2015; 10: 853–863.
25. Nix WD and Gao H. Indentation size effects in crystalline materials: a law for strain gradient plasticity. *J Mech Phys Solids* 1998; 46: 411–425.
26. Swadener JG, George EP and Pharr GM. The correlation of the indentation size effect measured with indenters of various shapes. *J Mech Phys Solids* 2002; 50: 681–694.
27. Han CS, Hartmaier A, Gao H, et al. Discrete dislocation dynamics simulations of surface induced size effects in plasticity. *Mater Sci Eng A* 2006; 415: 225–233.
28. Gong J and Li Y. Energy-balance analysis for the size effect in low-load hardness testing. *J Mater Sci* 2000; 35: 209–213.
29. Güder HS, Şahin E, Şahin O, et al. Vickers and Knoop indentation microhardness study of β -SiAlON ceramic. *Acta Phys Pol A* 2011; 120: 1026–1033.
30. Marwaha RK and Sahah BS. Microhardness studies on benzoic acid single crystals. *Cryst Res Technol* 1988; 23: K63–K65.
31. Şahin O, Uzun O, Kölemen U, et al. Dynamic hardness and reduced modulus determination on the (001) face of β -Sn single crystals by a depth sensing indentation technique. *J Phys Condens Matter* 2007; 19.